Int. J. Heat Mass Transfer. Vol. 13, pp. 667–680. Pergamon Press 1970. Printed in Great Britain

ENTRANCE REGION AND VARIABLE HEAT FLUX EFFECTS IN TURBULENT HEAT TRANSFER TO LIQUID METALS FLOWING IN CONCENTRIC ANNULI*

JOHN C. CHEN and W. S. YU
Brookhaven National Laboratory, Upton, New York, U.S.A.

(*Received* 26 *December* 1968 *and in revised form* 24 *September* 1969)

Abstract—An analytical solution was obtained for the turbulent entrance-region problem with a step-function heat flux distribution. Necessary eigenvalues, eigenfunctions, and series coefficients were evaluated from the characteristic equation by the method of Runge–Kutta. Calculated Nusselt numbers in the entrance region were found to be in general agreement with recent experimental measurements. The solution was then generalized to include cases of arbitrarily varying heat flux by means of Duhamel's integral, and sample results were obtained for cases of linear and sinusoidal heat flux distributions. Emphasis was placed on low-Prandtl-number fluids, though the solution is general and some sample calculations were made for fluids of moderate Prandtl numbers.

NOMENCLATURE

a, $r_2 - r_1$;
A, constant in sinusoidal heat flux function;
b, constant in linear heat flux function;
C_n, series coefficient in equation (12);
C_p, heat capacity;
F, heat flux function, as defined by equation (3);
G, function in temperature solution, as defined in equation (8);
k, molecular thermal conductivity;
k_e, total effective thermal conductivity;
L, period of sinusoidal heat flux form;
Pe, Peclet number $= 2a\rho V C_p/k$;
Pr, Prandtl number $= C_p\mu/k$;
q_1, heat flux at $r = r_1$;
q_2, heat flux at $r = r_2$;
Q, constant heat flux at $r = r_1$ for step-function case;
Nu, local Nusselt numbers for $\psi = 1$;
Nu', local Nusselt numbers for varying ψ;
r, radial coordinate;
r_1, radius of inner (core) tube;
r_2, radius of outer (shell) tube;
r_*, r_2/r_1;
R, $a/r_1 = r_* - 1$;
Re, Reynolds number $= 2a\rho V/\mu$;
T, temperature;
T_b, bulk temperatue;
T_0, inlet temperature;
T_w, wall temperature;
$T_{w.q}$, wall temperature, as defined by equation (20);
u, dimensionless local velocity $= v(y)/V$
v, axial velocity;
V, bulk average velocity;
x, $z/2a$;
x', defined by equation (20);
y, $(r - r_1)/a$;
Y_n, eigenfunction in equation (12);
z, axial coordinate.

Greek letters

β_n^2, eigenvalues in equation (12);
ε_h, turbulent eddy diffusivity of heat;
ε_m, turbulent eddy diffusivity of momentum;

* This work was performed under the auspices of the U.S. Atomic Energy Commission.

θ, dimensionless temperature $= [T - T_0]/[Qa/k]$;
θ_d, developed temperature solution;
θ_e, entrance-region temperature solution;
μ, viscosity;
ρ, density;
σ, dimensionless total diffusivity $= \frac{\rho}{\mu}\left(\frac{k}{\rho C_p} + \varepsilon_h\right)$;
ϕ, $(T_w - T_b)/(T_w - T_b)_d$;
ψ, ratio of heat to momentum diffusivities.

INTRODUCTION

HEAT TRANSFER to fluids flowing through annular passages is of practical importance and has been the subject of many studies in recent years [1–10]. In terms of theoretical analysis, the case of laminar flow is now well in hand with solutions available for the entrance region, the asymptotic (thermally developed) region, and for both constant and axially varying boundary conditions [7]. Analysis of heat transfer with turbulent flow in annuli is not nearly as complete. Only the thermally-developed, asymptotic case has been analyzed thoroughly for a wide range of radius ratios and Prandtl and Reynolds numbers [3, 5, 8–10]. For the entrance region problem, the most pertinent theoretical studies to date are those of Kays and Leung [9], Lee [10] and Quarmby and Anand [11]. Kays and Leung [9] utilized experimental measurements to deduce temperature solutions for four radius ratios and a number of Reynolds numbers. However, since their results were based on experimental measurements made with air, the complete solutions are available only for $Pr = 0{\cdot}7$. Lee [10] studied the classical entrance-region problem (with a step increase in heat flux), for the case of heat transfer from the core tube. Using a boundary-layer model and an assumed radial distribution of heat flux, he obtained only numerical solutions for the entrance-region Nusselt numbers at several radius ratios, Prandtl numbers and Reynolds numbers. For the more complex problem of axially varying heat flux, only the experimentally derived solution of Kays and Leung is available. As indicated in their paper [9], Kays and Leung's temperature functions may be utilized to obtain local Nusselt numbers for axially varying heat fluxes by the superposition technique, provided $Pr = 0{\cdot}7$ and Re and r_* are restricted to the values of their tests. Lee's [10] numerical solutions are limited entirely to the step-function boundary condition, and do not deal with the more general boundary condition of variable heat fluxes. Quarmby and Anand [11] has just recently presented a solution for the case of constant wall temperatures.

Thus, there appears to be a need for rigorous, general solutions for the problem of turbulent heat transfer in the entry-region of annuli, especially for the case of axially varying heat fluxes. Such analyses are needed most for fluids with low Prandtl numbers, (e.g. the liquid metals), for which the effects of variations in boundary conditions may be especially important.

This paper presents an exact, analytical treatment of the subject problem. Specifically, we considered the case of turbulent flow through concentric annuli with:

(a) fully developed turbulent flow
(b) uniform inlet temperature
(c) heat transfer from the inner (core) wall
(d) steady state
(e) heat flux arbitarily varying in the axial direction.

The approach was to first obtain a rigorous solution for the step-function, constant-heat-flux problem by means of the classical, orthogonal-expansion method previously utilized for heat transfer in tubes and between parallel plates [12, 13]. This type of solution was preferred since the eigenvalues and functions, once evaluated, could then be used to obtain solutions for the more general problem of axially varying heat flux. Emphasis was placed on low-Prandtl-number fluids, though the solution is generally applicable to, and some limited

results were obtained at, higher Prandtl numbers.

ANALYSIS

Figure 1 defines the geometry and coordinate system for the analysis. For a constant-property fluid in steady-state flow through an annulus, the energy transport equation may be written as

$$\rho C_p v \frac{\partial T}{\partial z} = \frac{1}{r}\frac{\partial}{\partial r}\left(r k_e \frac{\partial T}{\partial r}\right) \tag{1}$$

if axial symmetry exists. T and v are taken to be time-averaged temperature and axial velocity, respectively. The mean radial velocity is zero at all points for fully developed turbulent flow. and an entrance solution, θ_e, such that the

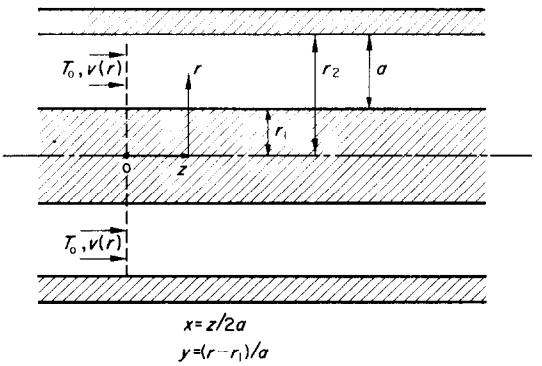

FIG. 1. Coordinate system.

In equation (1), k_e represents the total effective thermal conductivity, which includes both the molecular-conduction contribution and the turbulent, eddy-diffusion contribution:

$$k_e = k + \rho C_p \varepsilon_h. \tag{2}$$

The appropriate boundary conditions for the stated problem are:

q_1 = heat flux at inner wall

$$= -k\frac{\partial T}{\partial r}\bigg|_{r=r_1} = F(z) \tag{3}$$

$$q_2 = \text{heat flux at outer wall} = 0 \tag{4}$$

$$T(z = 0, r) = T_0. \tag{5}$$

(a) *Step-function case*

Consider first the simplest case where heat flux varies as a step function,

$$\left.\begin{aligned} q_1 &= F(z) = 0 \text{ for } z < 0 \\ &= Q, \text{ (a constant), for } z \geqslant 0. \end{aligned}\right\} \tag{6}$$

The dimensionless temperature solution is sought in two parts—a fully developed solution, θ_d, which is applicable in the region of large x, and an entrance solution, θ_e, such that the complete solution is given by:

$$\theta(x, y) = \theta_d(x, y) + \theta_e(x, y). \tag{7}$$

Due to its linearity, equation (1) is applicable to both θ_d and θ_e individually. It is evident that θ_d does not have to satisfy the initial condition at $x = 0$, and that θ_e approaches zero as $x \to \infty$.

By an analysis similar to that described in [12], the solution for θ_d is obtained as,

$$\theta_d(x, y) = \frac{8x}{Pe(2 + R)} + G(y) \tag{8}$$

where $G(y)$ represents the radial θ profile in the fully developed region. It can be shown that $G(y)$ is uniquely determined by the equations:

$$Re \cdot u(y) \cdot \frac{2}{Pe(2 + R)} = \frac{1}{1 + Ry} \times \frac{\mathrm{d}}{\mathrm{d}y}\left[\sigma(y) \cdot (1 + Ry)\frac{\mathrm{d}G}{\mathrm{d}y}\right]. \tag{9}$$

$$\frac{\partial G}{\partial y}\bigg|_{y=0} = -1 \tag{10}$$

$$\int_0^1 u(y) \cdot G(y) \cdot (1 + Ry)\,\mathrm{d}y = 0. \tag{11}$$

The solution for θ_e is obtained by separation of variables:

$$\theta_e(x, y) = \sum_{n=1}^{\infty} C_n Y_n(y) \exp\left[-\frac{4\beta_n^2}{Re}x\right] \tag{12}$$

where the eigen constant, B_n^2, and eigen functions, $Y_n(y)$, are determined from the characteristic equation,

$$\frac{\mathrm{d}}{\mathrm{d}y}\left[\sigma(y)\cdot(1+Ry)\cdot\frac{\mathrm{d}Y_n}{\mathrm{d}y}\right] + [u(y)\cdot(1+Ry)\cdot\beta_n^2]\,Y_n = 0 \quad (13)$$

and boundary conditions,

$$\left.\frac{\partial Y_n}{\partial y}\right|_{y=0} = \left.\frac{\partial Y_n}{\partial y}\right|_{y=1} = 0. \quad (14)$$

Due to the orthogonality property of the governing equations, the series coefficients, C_n, can be obtained from the relation

$$C_n = \frac{-\int_0^1 u(y)\cdot G(y)\cdot(1+Ry)\cdot Y_n\,\mathrm{d}y}{\int_0^1 u(y)\cdot(1+Ry)\cdot Y_n^2\,\mathrm{d}y}. \quad (15)$$

The complete temperature solution is thus,

$$\theta(x,y) = \frac{8}{(2+R)\,Pe}x + G(y) + \sum_{n=1}^{\infty} C_n Y_n(y)\exp\left[-\frac{4\beta_n^2}{Re}x\right] \quad (16)$$

It is of particular interest to know the local wall temperature, which is determined from equation (16) to be,

$$T_w(x, y=0) = T_0 + \frac{Qa}{k}\left[\frac{8x}{(2+R)\,Pe} + G(0) + \sum_{n=1}^{\infty} C_n Y_n(0)\exp\left[-\frac{4\beta_n^2}{Re}x\right]\right] \quad (17)$$

The local Nusselt number is then obtained as

$$Nu(x) = \frac{2aQ}{k(T_w - T_b)} = \frac{2}{G(0) + \sum_{n=1}^{\infty} C_n Y_n(0)\exp\left[-\frac{4\beta_n^2}{Re}x\right]}, \quad (18)$$

and the fully developed Nusselt number is found to be,

$$Nu(x=\infty) = \frac{2}{G(0)}. \quad (19)$$

(b) *Variable heat flux case*

Here, we allow the wall heat flux to be an arbitrary function of axial position:

$$q_1 = F(x) \qquad \text{for} \quad x \geqslant 0.$$

Due to the linearity of the governing energy equation (1), it is possible to use Duhamel's integral to extend the step-function solution to the case of variable heat flux. From equation (17), we have that the effect of a unit increase in heat flux ($Q = 1$), at position x', on the downstream wall temperature is

$$T_{w,q}(x, x') - T_0 = +\frac{a}{k}\frac{8(x-x')}{(2+R)\,Pe} + G(0) + \sum_{n=1}^{\infty} C_n Y_n(0)\exp\left[-\frac{4\beta_n^2}{Re}(x-x')\right]. \quad (20)$$

Applying Duhamel's theorem, the wall temperature at x, resulting from a variable heat flux, $q_1 = F(x')$, in the region $0 \leqslant x' < x$ is,

$$T_w(x) - T_0 = \int_0^x F(x')\cdot\frac{\partial}{\partial x}\left[T_{w,q}(x, x') - T_0\right]\mathrm{d}x'$$

whence,

$$T_w(x) = T_0 + \frac{4a}{k}\int_0^x F(x')\cdot\left\{\frac{2}{(2+R)\,Pe} - \frac{1}{Re}\sum_{n=1}^{\infty} C_n\beta_n^2 Y_n(0)\exp\left[-\frac{4\beta_n^2}{Re}(x-x')\right]\right\}\mathrm{d}x'. \quad (21)$$

The local bulk temperature is obtained by heat balance,

$$T_b(x) = T_0 + \frac{8a}{k(2+R)\,Pe}\int_0^x F(x')\,\mathrm{d}x'. \quad (22)$$

The local Nusselt number may then be determined to be:

$$Nu(x) = \frac{2a \cdot F(x)}{k[T_w(x) - T_b(x)]} = \frac{Re \cdot F(x)}{-2\int_0^x F(x') \cdot \sum_{n=1}^{\infty} C_n \beta_n^2 Y_n(0) \exp\left[-\frac{4\beta_n^2}{Re}(x - x')\right] dx'} \quad (23)$$

COMPUTATION

The temperature solution and the expression for local Nusselt numbers derived above constitute a rigorous solution to the subject problem. To utilize this solution a number of evaluation and computation steps are required, namely:

(a) specify the velocity distribution, $u(y)$;
(b) specify the diffusivity distribution, $\sigma(y)$;
(c) determine the $G(y)$ function;
(d) determine the eigenvalues, β_n^2, the eigen function, $Y_n(y)$, and the series coefficients, C_n;
(e) calculate $Nu(x)$ as desired for any $F(x)$ of interest.

A number of authors have presented either experimental data or correlations for the fully developed, turbulent velocity profile in concentric annuli [8, 9, 14–21]. Some disagreements still exist regarding the "correct" velocity profile and the radius of maximum velocity. For the present study, the empirical correlation suggested by Kays and Leung [9] was used to specify $u(y)$. This correlation was found to be in reasonable agreement with the experimental measurements of both Knudsen and Katz [16] and Brighton and Jones [14]. Levy's correlation [18] gives approximately the same velocity distribution. The procedures suggested by Rothfus *et al.* [15] or by Clump and Kwasnoski [19] may give slightly more accurate estimates of the velocity distribution. However, both these procedures required trial-and-error calculations and it was felt that for the purpose of this study, the small difference in the results did not warrant this additional complexity.

The total diffusivity, $\sigma(y) = \frac{\rho}{\mu}\left(\frac{k}{\rho C_p} + \varepsilon_h\right)$, is position dependent only because of variations in the turbulent diffusivity, ε_h. Fortunately, for liquid metals or other fluids of low Prandtl numbers, the turbulent diffusivity is small relative to molecular diffusivity in most cases; i.e.

$$\frac{k}{\rho C_p} > \varepsilon_h,$$

so that some latitude in the specification of ε_h is acceptable. Following common practice, one can write the thermal diffusivity in terms of the momentum diffusivity:

$$\varepsilon_h = \psi \varepsilon_m. \quad (24)$$

Rigorously speaking, ψ is dependent on Re, Pr, r_* and y [22]. However, this dependence is small for fluids of moderate Prandtl numbers, for which $\psi \cong 1$. For low Pr fluids where ψ may be significantly different from unity, the net effect is often still of only second order due to the relative importance of molecular conduction. In this study, sample results were obtained both for $\psi = 1$ and for ψ varying with radial position. For the radial distribution of ε_m, the expressions developed by Deissler [23] and Reichardt [24], as modified by Kays and Leung [9] for flow in concentric annuli, were used in the computations. The modified expressions successfully correlated the experimental data of Knudsen and Katz [16]. Again, the slight increase in accuracy that may have been attained by following the trial and error procedure of Rothfus *et al.* [15] was felt to be unnecessary for this problem.

Once $u(y)$ and $\sigma(y)$ have been specified, it becomes possible to determine the $G(y)$ function by numerical solution of equations (9)–(11). The eigenvalues, β_n^2, and eigenfunctions, $Y_n(y)$, were determined from equations (13) and (14) by the Runge–Kutta method. Even with the aid of a high-speed digital computer, this step required a substantial effort. To obtain sufficient

accuracy in the local Nusselt numbers for small values of x or for cases with rapidly varying wall heat flux, it was felt that one would require a minimum of five eigenvalues in the series expansion. Twenty terms, with 10 significant figures for both β_n^2 and $Y_n(y)$, were actually obtained and used in this study for all sample cases. The series coefficients, C_n, were then evaluated by equation (15).

With β_n^2, $Y_n(y)$ and C_n in hand, the local temperature, $\theta(x, y)$, and local Nusselt numbers, $Nu(x)$, for the turbulent entrance region with a step-function heat flux could be calculated from equations (16) and (18), respectively. Similarly, local Nusselt numbers could be calculated for the variable flux case by equation (23).

RESULTS AND DISCUSSION

The eigenvalues and functions were determined for fourteen sample cases, with the following ranges of variables:

Re: 10^4, 5×10^4, 10^5, $1{\cdot}7 \times 10^5$, 2×10^5
Pr: 0·005, 0·01, 0·023, 0·03, 0·06, 0·1, 0·7, 1, 5
r_*: 1·5, 2·5, 2·78, 4·0.

Since the primary interest of this study is in heat transfer with liquid metals, the majority of the sample calculations dealt with $Pr = 0{\cdot}005$, which is the Prandtl number for sodium at 800°F. Table 1 presents values of β_n^2 and $C_n \cdot Y_n(0)$, based on $\psi = 1$, inasmuch as these are the functions required to calculate Nusselt numbers. Due to space limitations, values are given only up to n of 6, while actually 20 eigen terms were evaluated and used in all calculations.

Figures 2–8 present results for the step-function (constant) heat flux case. Figure 2 illustrates the variations in local Nu for different Reynolds numbers, at $Pr = 0{\cdot}005$ and $r_* = 1{\cdot}5$. As anticipated, $Nu(x)$ decreases from infinity at $x = 0$ to asymptotically approach the fully developed value as $x \to \infty$. These results clearly indicate that the approach to the fully developed Nu is slower (longer thermal entry length) for higher Re. Also shown on this graph are the

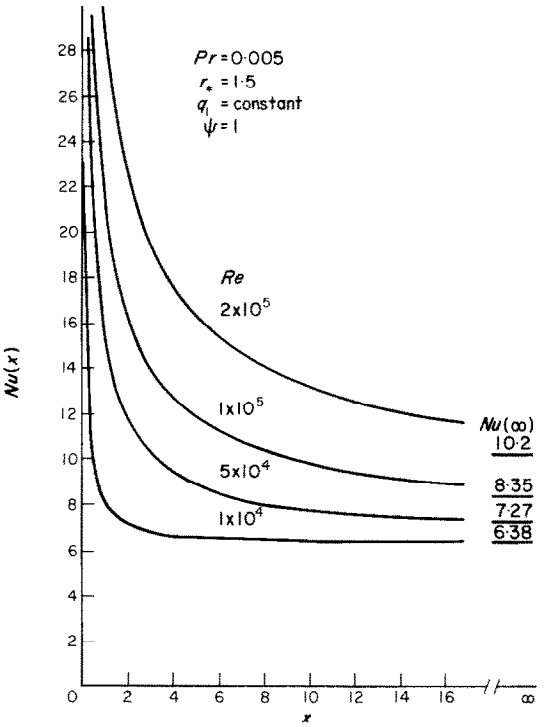

FIG. 2. Effect of Reynolds number on local Nusselt numbers.

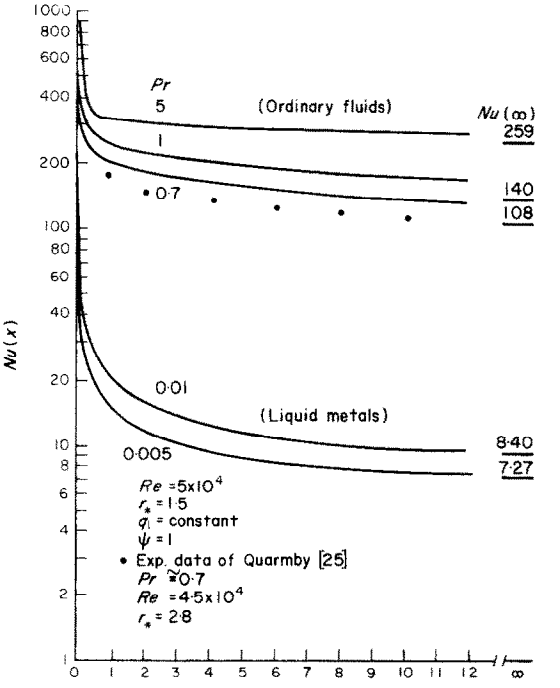

FIG. 3. Effect of Prandtl number on local Nusselt numbers.

Table 1. Eigenvalues and series coefficients

Pr	Re	r_2/r_1	n	β_n^2	$C_nY_n(0)$	n	β_n^2	$C_nY_n(0)$
			1	2701	−0·1492	4	39790	−0·01334
0·005	5×10^4	1·5	2	10330	−0·04439	5	61730	−0·007600
			3	22630	−0·02059	6	88540	−0·006676
			1	2815	−0·1294	4	39970	−0·01272
0·005	5×10^4	2·5	2	10470	−0·04125	5	61970	−0·007333
			3	22810	−0·01966	6	88780	−0·006338
			1	2971	−0·1042	4	40220	−0·01204
0·005	5×10^4	4·0	2	10670	−0·03684	5	62260	−0·007125
			3	23060	−0·01837	6	89100	−0·006070
			1	2329	−0·1716	4	34300	−0·01474
0·005	1×10^4	1·5	2	8819	−0·05113	5	53290	−0·008722
			3	19460	−0·02324	6	76470	−0·007413
			1	3152	−0·1288	4	46190	−0·01194
0·005	1×10^5	1·5	2	12120	−0·03838	5	71510	−0·007100
			3	26340	−0·01857	6	102500	−0·006005
			1	4017	−0·1021	4	58290	−0·01026
0·005	2×10^5	1·5	2	15530	−0·03089	5	89950	−0·006273
			3	33370	−0·01570	6	128700	−0·005328
			1	1630	−0·1253	4	23800	−0·01214
0·01	5×10^4	1·5	2	6259	−0·03782	5	36820	−0·007417
			3	13580	−0·01862	6	52740	−0·006334
			1	2275	−0·03653	4	29730	−0·005023
0·023	$1·7 \times 10^5$	2·78	2	8346	−0·01260	5	45480	−0·003138
			3	17400	−0·007463	6	64500	−0·002558
			1	897·5	−0·07705	4	12770	−0·007432
0·03	5×10^4	1·5	2	3464	−0·02345	5	19620	−0·004111
			3	7351	−0·01189	6	28030	−0·003272
			1	715·5	−0·04911	4	9972	−0·004759
0·06	5×10^4	1·5	2	2766	−0·01515	5	15240	−0·002501
			3	5781	−0·007955	6	21700	−0·001786
			1	639·5	−0·03303	4	8775	−0·003228
0·1	5×10^4	1·5	2	2471	−0·01040	5	13350	−0·001490
			3	5115	−0·005455	6	18970	−0·001043
			1	532·1	−0·006004	4	6916	−0·0008041
0·7	5×10^4	1·5	2	2034	−0·002150	5	10420	0·00001265
			3	4097	−0·0009184	6	14770	−0·0003053
			1	526·8	−0·004213	4	6820	−0·0005940
1·0	5×10^4	1·5	2	2013	−0·001529	5	10270	0·00000185
			3	4045	−0·006604	6	14540	−0·0002440
			1	518·0	−0·0008753	4	6661	−0·0001625
5·0	5×10^4	1·5	2	1977	−0·0003362	5	10010	−0·0003373
			3	3961	−0·0001635	6	14160	−0·0001047

developed Nusselt numbers, $Nu(\infty)$ calculated by equation (19).

The strong effect of Prandtl number on local Nu is shown in Fig. 3. These Nu were calculated for $Re = 5 \times 10^4$ and $r_* = 1{\cdot}5$. To interpret these results in terms of real fluids, note that the five sample Prandtl numbers are equal to those of the following fluids at the listed temperatures:

Pr	Fluid	Temperature F
0·005	sodium	800
0·010	sodium	250
0·7	air (1 atm)	212
1·0	water	340
5·0	water	94

Some experimental data obtained with air [25] are also shown in Fig. 3. These are seen to be approximately 5–10 per cent lower than the curve calculated for $Pr = 0{\cdot}7$. This difference seems reasonable in view of the slightly different Re and r_* values for the experimental (vs. calculation) conditions.

The effects of entrance-region and variable heat flux has often been taken to be more important for low-Prandtl-number fluids than for fluids with moderate or high Prandtl numbers [26]. Thus, for a given set of conditions, at a given axial position (x), one normally expects the ratio $Nu(x)/Nu(\infty)$ to increase with decreasing Pr. The present analysis indicates that this behavior is actually true only for certain ranges of the governing parameters. Figure 4 shows plots of $Nu(x)/Nu(\infty)$ vs. Pr at various values of x, for constant Re and r_*. It is seen that in the range of $Pr > 0{\cdot}1$, the entrance effect, as measured by increasing $Nu(x)/Nu(\infty)$, does indeed increase with decreasing Pr. However, further decreases of Pr below 0·1 shows $Nu(x)/Nu(\infty)$ passing through a maximum and then decreasing. Physically, this behavior can be attributed to two opposing factors. First decreasing Pr (increasing thermal conductivity) tends to increase the zone of influence of the wall so that the over-all temperature profile is more greatly affected by changes at the boundary. On the other hand, higher thermal conductivities tend to increase the speed of establishing thermal boundary layers, which would aid in the approach to fully developed conditions. Which of the two factors predominate would, of course, be dependent on the specifics of a given situation and would be influenced by the other independent variables: Re, x and r_*. For the conditions represented in Fig. 4, the entrance-region effect was determined to be most important for fluids with $(2 \times 10^{-2}) \leqslant Pr \leqslant (5 \times 10^{-1})$. It is interesting to note that Sleicher and Tribus [27] found a similar maxima effect in the variation of entry length with Pr for the case of turbulent flow in tubes with constant temperature boundary condition.

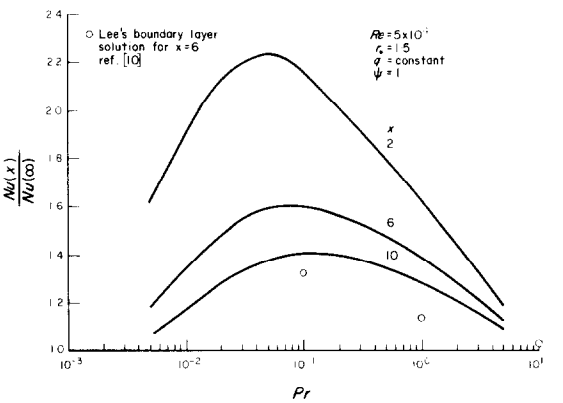

FIG. 4. Variation of entrance effect with Prandtl number.

The open circles on Fig. 4 represent Lee's results [10] from his boundary-layer solution for the same conditions, at $x = 6$. These are seen to be substantially lower than the comparable curve obtained in the present study. It is significant to note that the formal solution of Sparrow *et al.* [12] for the problem of turbulent flow in tubes also showed greater entrance effect than the boundary layer type of solution (per Deissler [28]). Sparrow *et al.* [12] noted that the boundary layer approach, which requires that either the temperature or the heat flux radial profile be assumed, may be more subject to error than the formal orthogonal-series type of solution. In the case of Lee's boundary-layer

solution for annuli, the assumed radial heat-flux distribution was based on an expression originally obtained for the fully-developed region, with slug flow. There is some uncertainty regarding the accuracy and effect of such an assumption for analysis of the entrance region.

The radius ratio, r_*, has a relatively minor effect on local Nusselt numbers. This is demonstrated in Fig. 5, where $Nu(x)$ is plotted vs. x

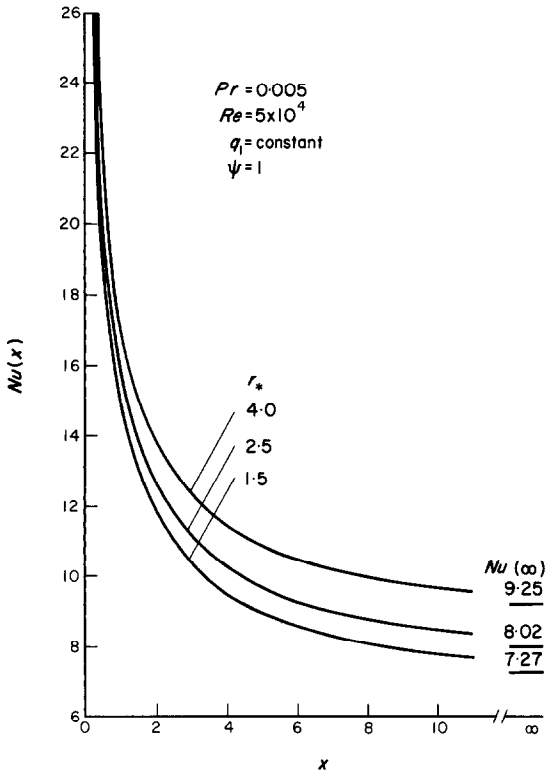

FIG. 5. Effect of radius ratio on local Nusselt numbers.

at three values of r_*, for $Pr = 0{\cdot}005$ and $Re = 5 \times 10^4$. It is seen that at these conditions, for $x > 1$, $Nu(x)$ changes no more than 22 per cent as the radius ratio is reduced by a factor of 2·7 (from 4·0 to 1·5). It should be noted that as r_* approaches unity, $Nu(x)$ should approach the values for the case of flow between parallel plates. At the other limit, as r_* approaches infinity, one would expect $Nu(x)$ to approach the values for external flow over a cylinder.

The analysis was compared with some recent experimental data of Nimmo *et al.* [29], and the results are shown in Fig. 6. The experimental

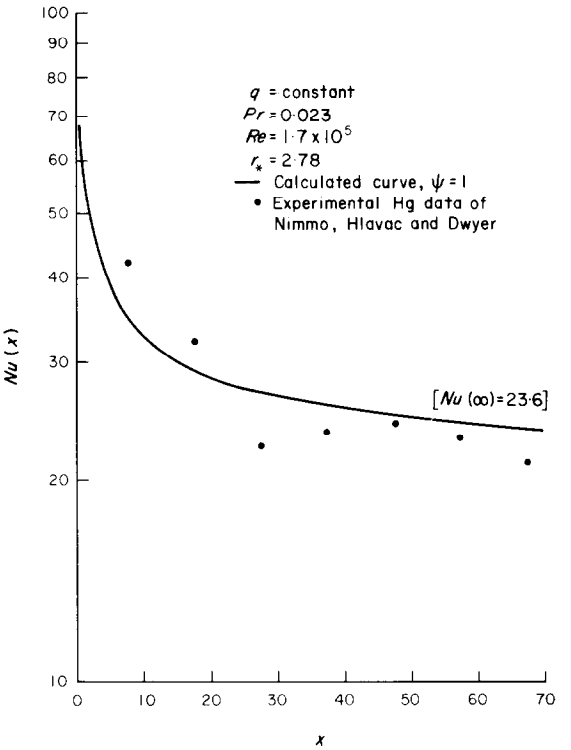

FIG. 6. Comparison of calculated and experimental Nusselt numbers.

measurements were made at a constant heat flux, using mercury as the test fluid. It should be noted that the test geometry was such that fluid-dynamic and thermal boundary layers developed *simultaneously*, so that the experimental Nu would be expected to be slightly greater than the calculated Nu at small values of x. In view of this limitation and the difficulties associated with making accurate heat transfer measurements in liquid metal systems, the agreement between calculated and measured Nu shown in Fig. 6 appears reasonable.

Figure 7 shows the effect of assuming non-unity diffusivity ratios, ψ, on the computed results. Of the various expressions that have been

proposed for estimating ψ as a function of radial position, those of Buyco [30] and Dwyer [31] are among the most recent and most applicable to liquid metals. Figure 7 shows $\left[\frac{Nu(x) - Nu'(x)}{Nu(x)}\right]$ for two sample cases, computed by:

(a) $\psi = 1$ (25)

(b) Buyco's expression

$$\psi = \frac{6}{\pi^2} Pr \frac{\varepsilon_m}{\nu} \left\{1{\cdot}1 - \exp\left[-\frac{\pi^2}{Pr(\varepsilon_m/\nu)}\right]\right\} \quad (26)$$

(c) Dwyer's expression

$$\psi = 1 - \frac{0{\cdot}2/Pr - 2{\cdot}0}{(\varepsilon_m/\nu)^{0{\cdot}9}} \quad (27)$$

where, $Nu(x)$ is calculated based on ψ given by equation (25) and $Nu'(x)$ is calculated based on ψ given by either equation (26) or equation (27).

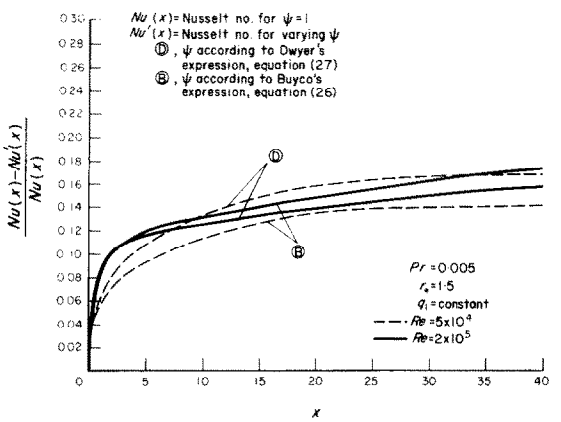

FIG. 7. Effect of diffusivity ratios on local Nusselt numbers.

As one would expect, the local Nu based on variable ψ are lower than the corresponding Nu for $\psi = 1$. For the cases considered, both Dwyer's and Buyco's expressions lead to Nusselt numbers which are approximately 0–18 per cent less than those for $\psi = 1$. The effect of non-unity diffusivity ratio is seen to be less important in the entry region than in the fully developed region.

The fully developed Nusselt numbers, $Nu(\infty)$, shown in the various figures were calculated by equation (19). A number of correlations for developed Nusselt numbers have been previously published and can be compared with equation (19). In 1962, Baker and Sesonske [32] published data and an empirical correlation based on measurements made with Na as NaK in a double-pipe heat exchanger. Seban [33] developed an expression for heat transfer to liquid metals flowing between parallel plates which can be used to estimate Nusselt numbers for annuli with small radius ratios. Most recently, Dwyer [31] presented a semi-empirical correlation which includes the effect of variable average ψ. These three correlations are compared with the present analysis in Fig. 8,

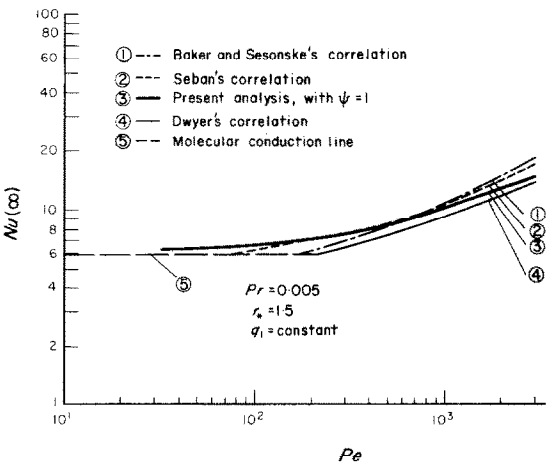

FIG. 8. Fully developed Nusselt numbers.

where the fully developed Nu is plotted against Péclét number for $r_* = 1{\cdot}5$ and $Pr = 0{\cdot}005$. Also shown in the figure is the Nusselt number for the limiting case of molecular conduction transfer, which is applicable at low Péclét numbers. It is seen that the present analysis is in general agreement with these empirical correlations. The calculated Nusselt numbers approach the values predicted by Dwyer's correlation at high Péclét numbers and approach the molecular-conduction value at low Péclét numbers.

The last three figures present results for cases of axially varying heat flux. Figure 9 illustrates the variations of the local Nusselt numbers for linearly changing heat flux, where $q_1 = 1 + bx$. With increasing heat flux ($b > 0$), $Nu(x)$ is seen to be higher than the corresponding values for the constant flux case ($b = 0$). For

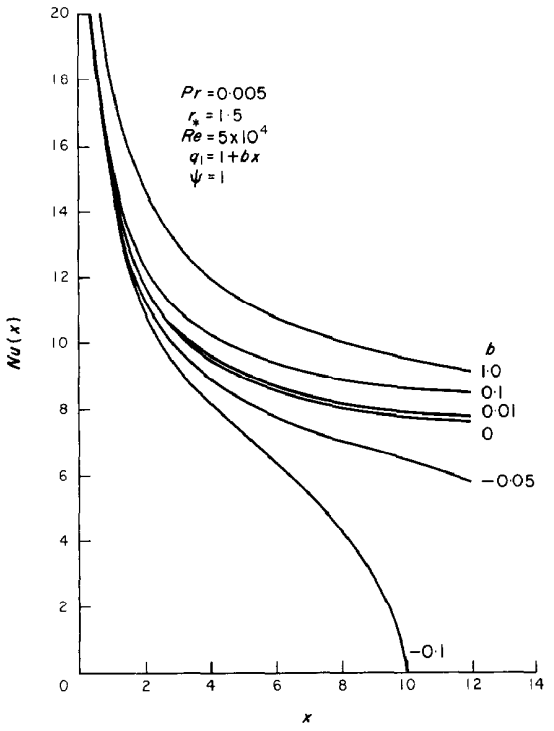

FIG. 9. Local Nusselt numbers for linearly varying heat flux.

the conditions of this sample case, the difference is seen to be significant for $b > 0{\cdot}01$. The effect is even more pronounced for decreasing heat fluxes ($b < 0$). For the conditions considered, it is seen that with b equal to $-0{\cdot}05$, there is a decrease of approximately 25 per cent in $Nu(x)$ from the constant-flux value, at $x = 12$. With negative values of b, q_1 becomes zero at $x = 1/b$ where $Nu \to 0$. This is illustrated in Fig. 9 by the curve for $b = -0{\cdot}1$ which approaches zero at $x = 10$ equivalent diameters.

Figure 10 presents local Nusselt numbers for cases of sinusoidal heat flux variations. Zero amplitude ($A = 0$) corresponds to the base case of step-function heat flux. For non-zero amplitude ($A > 0$), one finds the local Nu to be first greater than, and then less than, the base case Nu as x increases from 0 to L. The cross-over point, where the local Nu is equal to that for the base case, is seen to be in the region of $x \cong 0{\cdot}7L$ for all cases shown.

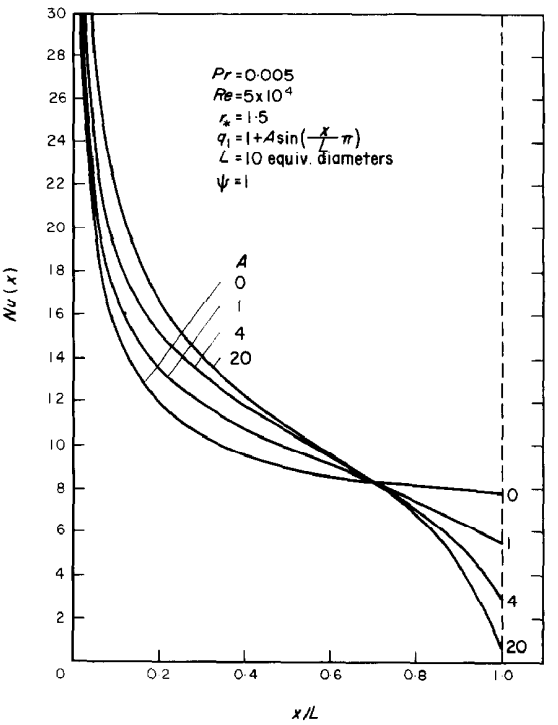

FIG. 10. Local Nusselt numbers for sinusoidal heat flux.

From the designers' point of view, it is important to know the error that would result from neglecting the effect of axial variations in heat flux. For example, in nuclear reactor cores where heat flux profiles are often of a sinusoidal shape, one would like to know the error in $(T_w - T_b)$ that would occur should the thermal design be based on the simple, fully developed Nu corresponding to the constant flux case. The temperature difference based

on this simple, approximate design is

$$(T_w - T_b)_d = \frac{2a}{Nu(\infty)\,k} \cdot F(x) \qquad (28)$$

where $Nu(\infty)$ equals fully developed Nu for constant flux case. The actual temperature difference, based on the present rigorous solution is

$$(T_w - T_b) = \frac{2a}{Nu(x)\,k} \cdot F(x) \qquad (29)$$

where $Nu(x)$ is evaluated from equation (23). Figure 11 shows plots of the ratio $\phi = (T_w - T_b)/(T_w - T_b)_d$ for a heat flux of $q_1 = 1 + 20 \sin[(x/L)\pi]$. Curves are presented for two values of the period L. Note that $\phi = 1$ indicates zero error, $\phi < 1$ indicates $(T_w - T_b)_d$ is a conservative design, and $\phi > 1$ indicates $(T_w - T_b)_d$ is an inadequate design. In the two examples shown, it is seen that the simple design is conservative for $0 < x < 0{\cdot}67L$, then becomes increasingly more inadequate as $x \to L$. At $x \cong 0{\cdot}9\,L$, the temperature difference estimated by the simple design is in error by ≈ 50 per cent. The real consequence of this error would be affected by specific design parameters since (a) the error is greatest in the region of decreasing heat flux where temperature differences may be small in any case, but on the other hand, (b) the greatest error is in the exit region where the fluid would be hottest and one may be especially concerned with a maximum temperature limitation on the heating surface.

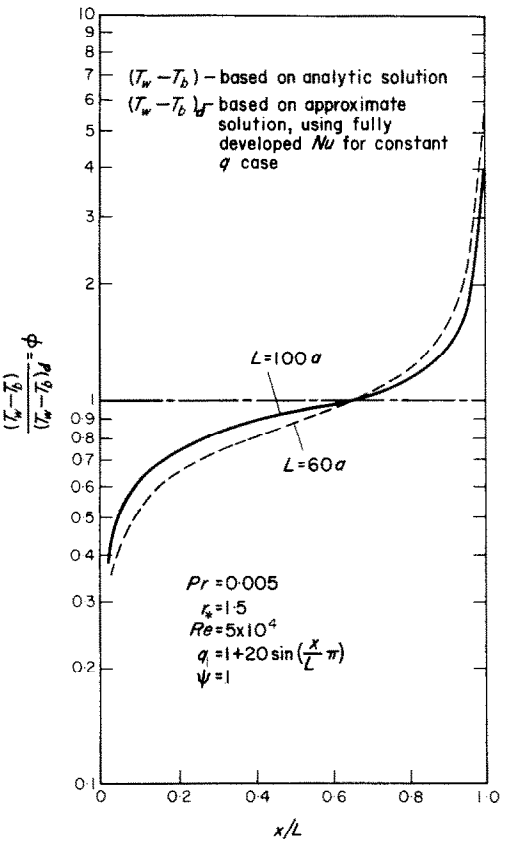

FIG. 11. Temperature difference for sinusoidal heat flux.

REFERENCES

1. W. C. REYNOLDS, R. E. LUNDBERG and P. A. MCCUEN, Heat transfer in annular passages—General formulation of the problem for arbitrarily prescribed wall temperatures or heat fluxes, *Int. J. Heat Mass Transfer* **6**, 483–493 (1963).
2. O. E. DWYER, On the transfer of heat to fluids flowing through pipes, annuli and parallel plates, *Nucl. Sci. Engng* **17**, 336–344 (1963).
3. O. E. DWYER and P. S. TU, Unilateral heat transfer to liquid metals flowing in annuli, *Nucl. Sci. Engng* **15**, 58–68 (1962).
4. W. S. YU and O. E. DWYER, Heat transfer to liquid metals flowing turbulently in eccentric annuli, *Nucl. Sci. Engng* **24**, 105–117 (1966).
5. O. E. DWYER, Equations for bilateral heat transfer to a fluid flowing in a concentric annulus, *Nucl. Sci. Engng* **15**, 52–57 (1963).
6. R. P. STEIN, Liquid metal heat transfer, *Advances in Heat Transfer* Vol. 3, pp. 101–174. Academic Press, New York (1966).
7. R. E. LUNDBERG, P. A. MCCUEN and W. C. REYNOLDS, Heat transfer in annular passages—Hydrodynamically developed laminar flow with arbitrarily prescribed wall temperatures or heat fluxes, *Int. J. Heat Mass Transfer* **6**, 495–529 (1963).
8. R. G. DEISSLER and M. F. TAYLOR, Analysis of fully developed turbulent heat transfer and flow in an annulus with various eccentricities, NACA-TN3451 (1955).
9. W. M. KAYS and E. Y. LEUNG, Heat transfer in annular passages—Hydrodynamically developed turbulent flow with arbitrarily prescribed heat flux, *Int. J. Heat Mass Transfer* **6**, 537–557 (1963).
10. Y. LEE, Turbulent heat transfer from the core tube in thermal entrance regions of concentric annuli, *Int. J. Heat Mass Transfer* **11**, 509–522 (1968).

11. A. QUARMBY and R. K. ANAND, Turbulent heat transfer in concentric annuli with constant wall temperatures, *ASME Paper* 69-HT-51 (1969).
12. E. M. SPARROW, T. M. HALLMAN and R. SIEGEL, Turbulent heat transfer in the thermal entrance region of a pipe with uniform heat flux, *Appl. Sci. Res.* 7A, 37–52 (1958).
13. A. P. HATTON and A. QUARMBY, The effect of axially varying and unsymmetrical boundary conditions on heat transfer with turbulent flow between parallel plates, *Int. J. Heat Mass Transfer* **6**, 903–914 (1963).
14. J. A. BRIGHTON and J. B. JONES, Fully developed turbulent flow in annuli, *J. Bas. Engng* **D86**, 835–844 (1964).
15. R. R. ROTHFUS, W. K. SARTORY and R. I. KERMODE, Flow in concentric annuli at high Reynolds numbers, *A.I.Ch.E. Jl* **12**, 1086–1091 (1966).
16. J. G. KNUDSEN and D. L. KATZ, Velocity profiles in annuli, *Proc. First Midwestern Conf. on Fluid Mechanics*, Illinois (1950).
17. A. ROBERTS, A comment on the turbulent flow velocity profile in a concentric annulus, *Int. J. Heat Mass Transfer* **10**, 709–712 (1967).
18. S. LEVY, Turbulent flow in an annulus, *J. Heat Transfer*, **89C**, 25–21 (1967).
19. C. W. CLUMP and D. KWASNOSKI, Turbulent flow in concentric annuli, *A.I.Ch.E. Jl* **14**, 164–168 (1968).
20. V. K. JONSSON and E. M. SPARROW, Turbulent diffusivity for momentum transfer in concentric annuli, *J. Bas. Engng* **88**, 550–552 (1966).
21. A. QUARMBY, An experimental study of turbulent flow through concentric annuli, *Int. J. Mech. Sci.* **9**, 205–221 (1967).
22. O. E. DWYER, Eddy transport in liquid metal heat transfer, *A.I.Ch.E. Jl* **9**, 261–268 (1963).
23. R. G. DEISSLER, Analysis of turbulent heat transfer, mass transfer and fluid friction in smooth tubes at high Prandtl and Schmidt numbers, NACA Report 1210 (1955).
24. H. REICHARDT, Complete representation of turbulent velocity in a smooth pipe, *Z. Angew. Math. Mech.* **31**, 208 (1951).
25. A. QUARMBY, Some measurements of turbulent heat transfer in the thermal entrance region of concentric annuli, *Int. J. Heat Mass Transfer* **10**, 267–276 (1967).
26. W. M. KAYS, *Convective Heat and Mass Transfer*, pp. 188, 189, 193. McGraw-Hill, New York (1966).
27. C. A. SLEICHER JR. and M. TRIBUS, Heat transfer in pipe with turbulent flow and arbitrary wall-temperature distribution, *Trans. Am. Soc. Mech. Engrs* **79**, 789–797 (1957).
28. R. G. DEISSLER, Turbulent heat transfer and friction in the entrance regions of smooth passages, *Trans. Am. Soc. Mech. Engrs* 77, 1221–1233 (1955).
29. B. NIMMO, P. HLAVAC and O. E. DWYER, Experimental study of heat transfer to turbulent flow of mercury in concentric annuli, to be published.
30. E. H. BUYCO, Heat and momentum transfer in liquid metals, Ph.D. Thesis Purdue University, Lafayette, Indiana (1961).
31. O. E. DWYER, Liquid-metal heat transfer, Manuscript for Chapter 5 of the 1968 Edition of the sodium and NaK supplement to the Liquid Metals Handbook, p. 7 and p. 33 (1968).
32. R. A. BAKER and A. SESONSKE, Heat transfer in sodium–potassium alloy, *Nucl. Sci. Engng* **13**, 283 (1962).
33. R. A. SEBAN, Heat transfer to a fluid flowing turbulently between parallel walls with asymmetric wall temperatures, *Trans. Am. Soc. Mech. Engrs* **72**, 789–795 (1950).

EFFETS DE LA RÉGION D'ENTRÉE ET DU FLUX DE CHALEUR VARIABLE SUR LE TRANSPORT DE CHALEUR TURBULENT VERS DES MÉTAUX LIQUIDES S'ÉCOULANT DANS DES CONDUITES ANNULAIRES CONCENTRIQUES

Résumé—Une solution analytique a été obtenue pour le problème de la région d'entrée en turbulent avec une distribution de flux de chaleur en échelon. Les valeurs propres, les fonctions propres et les coefficients de séries nécessaires ont été évalués à partir de l'équation caractéristique par la méthode de Runge–Kutta.

Les nombres de Nusselt calculés dans la région d'entrée étaient en accord général avec des mesures expérimentales récentes. La solution a été alors généralisée pour comprendre les cas d'un flux de chaleur variant arbitrairement, au moyen de l'intégrale de Duhamel, et des résultats d'exemples ont été obtenus pour les cas de distributions de flux de chaleur linéaire et sinusoïdale. On a insisté sur les fluides à faibles nombres de Prandtl, bien que la solution soit générale et quelques calculs d'exemples ont été faits pour des fluides à nombres de Prandtl modérés.

EINFLÜSSE DES HYDRODYNAMISCHEN EINLAUFS UND DER VERÄNDERLICHEN WÄRMESTROMDICHTE AUF DEN WÄRMEÜBERGANG BEI TURBULENTER STRÖMUNG VON FLÜSSIGEN METALLEN IN KONZENTRISCHEN RINGRÄUMEN

Für das Problem des turbulenten Einlaufgebietes bei stufenförmiger Verteilung der Wärmestromdichte wurde eine analytische Lösung gefunden. Die notwendigen Eigenwerte, Eigenfunktionen und Serien-koeffizienten wurden aus der charakteristischen Gleichung mit der Methode von Runge–Kutta ermittelt. Die berechneten Nusselt-Zahlen im Einlaufgebiet stimmen im allgemeinen mit neueren experimentellen Messungen überein. Die Lösung wurde dann mit Hilfe des Duhamel'schen Integrals

erweitert, sodass auch Fälle mit beliebiger Wärmestromverteilung eingeschlossen sind. Als Beispiele wurden die Ergebnisse für lineare und sinusförmige Wärmestromverteilungen berechnet. Besonders berücksichtigt wurden Flüssigkeiten mit kleiner Prandtlzahl, obwohl die Lösung allgemein gilt. Einige Rechnungen wurden für Flüssigkeiten mit mittleren Prandtl-Zahlen durchgeführt.

ВЛИЯНИЕ ВХОДНОГО УЧАСТКА И ПЕРЕМЕННОГО ТЕПЛОВОГО ПОТОКА НА ТУРБУЛЕНТНЫЙ ПЕРЕНОС ТЕПЛА ПРИ ТЕЧЕНИИ ЖИДКИХ МЕТАЛЛОВ В КОНЦЕНТРИЧЕСКИХ КАНАЛАХ

Аннотация—Получено аналитическое решение задачи турбулентного течения во входной области при распределении теплового потока по ступенчатому закону. Из характеристического уравнения рассчитаны с помощью метода Рунге-Кутта соответствующие собственные значения, собственные функции и коэффициенты рядов. Найдено, что расчетные значения критериев Нуссельта во входной области согласуются с полученными в последнее время данными экспериментальных измерений. С помощью интеграла Дюамеля решение обобщено на случай произвольно изменяемого теплового потока; получены результаты для линейного и синусоидального распределений теплового потока. Особое внимание обращалось на жидкости с низкими значения критерия Прандтля, хотя решение получено в общем виде, и проведены некоторые расчеты для жидкостей с умеренными значениями критерия Прандтля.